1
Dynamical and synchronization properties of delay-coupled lasers

C.M. Gonzalez, M.C. Soriano, M.C. Torrent, J. Garcia-Ojalvo, I. Fischer

1.1
Motivation: Why coupling lasers?

For some decades already, people have optically coupled semiconductor lasers with each other. Initially, the main motivation has been to superpose the emission of several lasers coherently, thereby boosting the output power. Different strategies have been followed, like injection locking high-power lasers with low-power coherent seed lasers, or to build laser arrays of edge-emitting lasers with laterally coupled lasers (see e.g. [1] and references therein). Later also 2-dimensional arrays of Vertical-Cavity Surface-Emitting Lasers (VCSELs) have been realized [1]. In the injection locking approach the coupling was mostly unidirectional and via the coherent optical field. In the case of laser arrays, the coupling can originate from different mechanisms, including coupling via a shared carrier reservoir and/or the spatial overlap of the optical fields. In either case the coupling times have been negligible or irrelevant for the observed behavior. Nevertheless, besides the intended injection-locked stable emission, both configuration also exhibited dynamical instabilities in the laser emission. For an overview of the history and the physics of injection locking instabilities please see [2]. The laterally coupled laser arrays can also exhibit dynamical instabilities (see e.g. [3, 4]). Comparing the emission of the individual stripes in the laser arrays, Winful et al. demonstrated one of the first examples for the possibility to synchronize deterministic chaos [5]. In 1997 Hohl et al. found that weakly coupling two nonidentical edge-emitting lasers face-to-face at a significant distance could lead not only to locking of their optical frequencies, but also to the synchronization of their relaxation oscillations, therefore affecting their dynamical behavior [6]. They found that the coupled lasers can exhibit localized synchronization characterized by low amplitude oscillations in one laser and large oscillations in the other. The laser intensities exhibited periodic or quasi-periodic oscillations. A few years later, Heil et al. and Fujino et al. found, that the non-negligible delay in the coupling of face-to-face, mutually coupled lasers induces characteristic instabilities in their emission dynamics and particular synchronization properties [7, 8]. This has inspired many studies on the influence of delayed coupling on laser dynamics, as well as delay-coupled sys-

tems in general. One key criteria for the classification of the dynamical behavior is the amount of the coupling delay. Qualitatively different behavior has been found for the cases of short [9] and long delays[7]. If the coupling delay τ is of the same order as the relaxation oscillation period τ_{RO} of the laser ($\tau \sim \tau_{RO}$), it is refered to as the *short delay regime*. If $\tau \gg \tau_{RO}$, it is denoted as the *long delay regime*. In the following we concentrate on the long delay regime. This chapter covers aspects of delay-induced instabilities, synchronization properties, modulation characteristics, influence of noise and the potential application of delay-coupled lasers.

1.2 Dynamics of two mutually delay-coupled lasers

1.2.1 Dynamical instability

Starting point for the study of delay-coupled lasers has been the configuration of two longitudinally delay-coupled semiconductor lasers in the long delay regime. A sketch of this configuration is depicted in Figure 1.1.

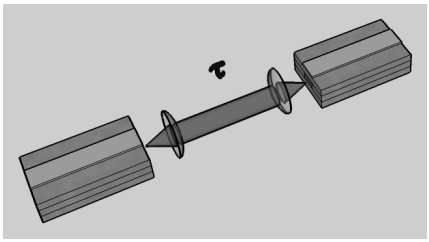

Figure 1.1 Two face-to-face delay-coupled semiconductor lasers (BETTER FIGURE?)

The long delay regime, defined by $\tau \gg \tau_{RO}$, is typically represented by geometric coupling distances of $l > 30$cm, corresponding to coupling delays of $\tau > 1$ns. We first consider the symmetric situation, meaning very similar lasers, adjustment of their wavelengths, identical operating conditions and symmetric bidirectional coupling. In [7] it has been found that the delayed coupling induces chaotic intensity dynamics on time scales ranging from sub-nanoseconds to microseconds. Figure 1.2 depicts a typical intensity time series of one of the mutually coupled lasers.

The dynamics resembles the dynamics found for delayed optical feedback. In some sense, these studies can be seen as an extension of the investigations of lasers with delayed feedback. The dynamics comprises similar Low Frequency Fluctuation (LFF) behavior. However, here it does not originate from passive feedback, but from delayed coupling due to the respective other laser. HERE MORE, PLEASE! (Miguel?)

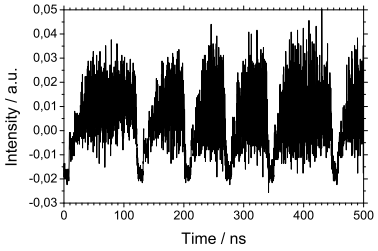

Figure 1.2 Intensity dynamics induced by mutual delayed coupling under symmetric conditions

1.2.2 Instability of isochronous solution

As a next step the intensity fluctuations of the two lasers have been compared with respect to each other. Figure 1.3 depicts the intensity dynamics of both lasers.

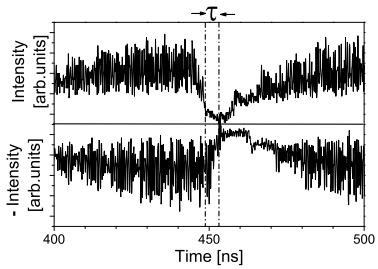

Figure 1.3 Comparison of the intensity dynamics of two delay-coupled lasers under symmetric conditions

For ease of comparison the second time series is vertically flipped. The two lasers exhibit correlated power dropouts and also correlated sub- nanosecond oscillations. However, these oscillation do not occur at the same time. The maximum correlation peak - reaching values of $C > 0.9$ - is obtained for a relative time shift, roughly given by τ or $-\tau$. Although the configuration is completely symmetric, the behavior is not. The lasers are not identically synchronized and show different temporal dynamics. They exhibit a form of generalized synchronization in which their behaviors are determined by the dynamics of the respective other laser, but how the dynamics between the two lasers relates to each other could not been identified yet. It is not given by a simple functional relationship. The maxima in the cross–correlation

function occurring at $+/-\tau$ indicate that one laser follows the respective other laser with a delay, however only showing similar, not identical, dynamics. Therefore, this type of generalized synchronization has also been referred to as leader–laggard type synchronization. While for completely symmetric conditions leader and laggard role emerge spontaneously and can even change in time, the role can also be externally controlled by introduction of slight asymmetries. One way to achieve this is by introducing a relative spectral detuning of the emission of the two lasers. Already for nominal detunings of only about 1GHz, being small to typical optical locking ranges of larger than 10 GHz, the leader and laggards role can be fixed. For edge–emitting lasers the laser with higher frequency becomes the leader in the dynamics [7, 10].

The emission dynamics of delay–coupled laser configurations – here in particular for two mutually delay–coupled lasers – can be modeled (assuming single solitary laser mode emission and low to moderate coupling) via a set of rate equations, resembling the Lang–Kobayashi equations [11] for the laser with feedback:

$$dotE_{1,2}(t) \quad = \quad \mp i\Delta E_{1,2} + \frac{1}{2}(1-i\alpha)\left[g_{n,i}n_i\right]E_{1,2} + \kappa_c E_{2,1}(t-\tau)\,, \qquad (1.1)$$

with κ_c being the coupling strength. E represents the slowly varying electric fields around the symmetric reference frame $(\Omega_2+\Omega_1)/2$, and Δ the detuning of the lasers in this reference frame. ($\Omega_{1,2}$ is the free running optical frequency of laser 1 and 2, respectively. The complementary equations for the excess carrier densities n_i read:

$$\dot{n}_i = (p-1)\frac{I_{th,i}}{e} - \gamma_e n_i - \Big(\Gamma_0 + g_{n,i}n_i(t)\Big)\|E_i\|^2\,, \qquad (1.2)$$

where, as before, $E_i(t)$ refers to the optical field generated by laser i and $g_{n,i}$ the differential gain of laser i. $I_{th,i}$ is the bias current at the solitary threshold of laser i, e is the electron charge, and p the pump parameter. $\|\cdots\|$ denotes the amplitude of the complex field.

Only from the experimental studies, one might assume that asymmetries in the setup or laser equations are the origin of the symmetry breaking, resulting in the observed leader–laggard behavior. This can be tested in the modeling, where one can choose perfectly symmetric conditions. As a result of the modelling, the same leader–laggard behavior is being found, corresponding to the generalized synchronization solution. Still, due to the symmetry of the system a symmetric solution has to exist, and in the modeling one can even prepare the system to start in this solution. Without noise, the system might even prevail inthis state for some time, however, as soon as one laser experiences a tiny perturbation, the system escapes to the generalized synchronized solution. The symmetric solution is unstable. This is shown in Figure 1.4.

Remarkably, this behavior, that the symmetric, isochronously synchronized solution is unstable in delay–coupled oscillators, holds not only for the chosen parameter conditions, but for all considered parameter situations and even for a large class of delay–coupled oscillators in general. It is only recently, that this general property has been understood [**? ?**].

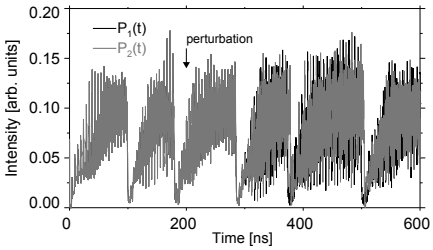

Figure 1.4 Intensity dynamics of two mutually delay–coupled lasers, obtained by modelling. At $t = 0$ the system is prepared in the isochronously synchronized state. At $t = 200$ a small perturbation is applied, resulting in the emergence of the leader–laggard state. courtesy of Claudio Mirasso.

1.3 Properties of Leader–Laggard synchronization

1.3.1 Emergence of Leader–Laggard Synchronization

As we have seen above, when two mutually coupled lasers operate have the same optical frequency, they synchronize with a lag, with a random change in the leader and laggard role. To understand the emergence of this symmetry breaking in the system, one can analyze the transition from unidirectional to bidirectional injection. This can be accomplished, for instance, with the experimental setup shown in the left panel of Fig. 1.5, in which the directionality of the coupling is varied in a controlled way, by separating the coupling path into two unidirectional paths and adding a neutral-density filter of varying transmittance to one of the paths. This allows one to see the transition from stable unidirectional injection to chaotic synchronization with a leader in the dynamics, and how this chaotic lag synchronization arises in the system.

In the unidirectional case the receiver laser (LD2) is stable at very low injection levels, with an optical power close to that of the emitter laser. When the (unidirectional) coupling is increased, the receiver laser goes from stable to oscillatory output. This oscillation becomes more and more unstable if the coupling is increased further, or by adding a reverse injection. When we depart from the unidirectional coupling state by gradually increasing the injected light coming from the reverse path, chaos arises in the system, with a clear symmetry breaking introduced by the time delay of the coupling paths.

The transition to chaos can be observed in the output intensities of the two lasers. The right panel of Fig. 1.5 shows the time traces of the two lasers (LD1 at the top and LD2 at the bottom) and the corresponding cross-correlation functions for increasing back injection. In the case of purely unidirectional injection [Fig. 1.5(a,b)] the emitter laser is naturally stable, and the receiver laser exhibits small oscillations as a result of the injection. The respective cross-correlation function has its maximum

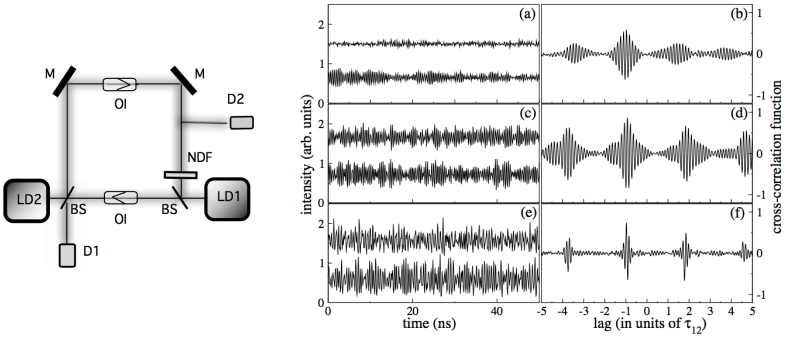

Figure 1.5 Left panel: experimental setup to examine the emergence of lag synchronization. Two lasers LD1 and LD2 are optically coupled through two unidirectional pathways running in opposite directions. A neutral-density filter in the path from LD2 to LD1 allows to tune the coupling from purely unidirectional from LD1 to LD2, to purely bidirectional. Right panel: (a,c,e) output intensities of LD1 (top) and LD2 (bottom) and the corresponding cross-correlation functions (b,d,f) for increasing back injection from LD2 to LD1 (from top to bottom).

at $-\tau_{1,2}$ (the flight time from LD1 to LD2). When the back injection is nonzero but small, the cross-correlation function reveals a quasi-periodic state due to the very high asymmetry in the couplings. The highest peak appears at $-\tau_{1,2}$, but several higher harmonics occur at lags $\tau_{1,2} + \tau_{2,1}$. Quasi-periodicity is revealed by growing peaks at those lags in the cross-correlation function. The chaotic dynamics typical of symmetric coupling is observed in the weakly assymmetric coupling case [Fig. 1.5(e,f)], and is characterized by a quick decrease to zero of the cross-correlation function away from its maximum. The difference in the rates at which the envelope of the cross-correlation peak decays characterizes the transition from a quasi-periodic to a chaotic behavior. These results show that the symmetry-breaking behavior underlying the leader-laggard dynamics [7] emerges from a quasi-periodic state that later transforms into a chaotic state with a well defined leader in the dynamics. The quasi-periodic state is characterized by out-of-phase synchronized outputs, with a cross-correlation function exhibiting a clear maximum at $-\tau_{1,2}$, and secondary peaks at a distance equal to the sum of the external cavities, while in the chaotic case the secondary peaks suffer a loss of correlation.

1.3.2
Control of lag synchronization

When the output of a semiconductor laser with feedback, operating in the LFF regime, is introduced into a second laser, power dropouts are also induced in the latter, provided the two lasers are similar enough in their physical properties. The dropouts are synchronized between the two lasers and, in general, the emitter laser leads the dy-

namics (i.e. the dropouts in the emitter precede those in the transmitter) [12, 13] with a time lag equal to the coupling time. If the coupling and feedback strengths are tuned such that the total injection (feedback + coupling) is equal for the two lasers, and if the feedback time is larger than the coupling delay, the emitter laser can anticipate the receiver [14]. This synchronization state is, nevertheless much less common and more difficult to reach than the usual lag synchronization state discussed here. Interestingly, a similar dynamics is observed in the case of two *bidirectionally* coupled lasers, even in the absence of an external mirror, as we have seen above. We remind the reader that when the two lasers have the same frequencies, the leader and laggard roles alternate randomly between the two lasers, while in the presence of frequency detuning the laser with higher frequency is the one leading the dynamics, again with a time lag equal to the coupling time. In the bidirectional case, a well defined leader also exists when one of the lasers is subject to feedback [15]; this behavior can again be attributed to the existence of a frequency detuning between the lasers, which is in this case induced by the feedback itself [16].

A question is then how is the transition between the unidirectional and bidirectional coupling schemes. To that end, one can use the experimental setup shown in the left panel of Fig. 1.6. In this scheme two semiconductor lasers, one of them subject to optical feedback from an external mirror, are coupled optically via two distinct paths through which light is made to travel in opposite directions with suitable optical isolators. The directionality of the coupling can be varied in a controlled way by tuning a neutral-density filter in one of the two paths.

The right panel of Fig. 1.6 shows the dynamical behavior of this system when coupling varies from purely unidirectional to purely bidirectional. In the absence of coupling from any of the two paths laser LD2 is stable, while laser LD1 operates in the LFF regime due to the optical feedback from the external mirror M. When a sufficient amount of light from LD1 is injected into LD2, the latter exhibits power dropouts as well, following those of LD1 with a certain time lag (see plot a in the right panel of Fig. 1.6). The time lag can be determined by comparing the times at which synchronized power dropouts occur in the two lasers. A histogram of the time differences between synchronized power dropouts corresponding to this regime is shown in plot b. The lag is calculated as the difference between the dropout times in LD1 and LD2. Therefore, a negative value corresponds to an *advance* of LD1 over LD2, as expected and evident from the vertical dashed lines in plot a. Intuitively, this lag is produced by the time needed by the light of one laser to affect the dynamics of the other one. We note that another synchronized state is possible in this setup, in which the lasers are synchronized at zero-lag (provided the feedback and coupling times are equal) [18], but this requires a very careful tuning to make the coupling and feedback strengths equal, and extremely similar lasers [12]; this regime is not shown here.

When the light emitted from LD2 is allowed to reach LD1, it becomes possible to control the strength of that coupling, varying the transmittivity of filter F2, while keeping the amount of light injected from LD1 into LD2 constant. Plot c in the right panel of Fig. 1.6 shows that for moderate transmittivities the situation does not change much with respect to the purely unidirectional case (LD1 leads the dynamics a time

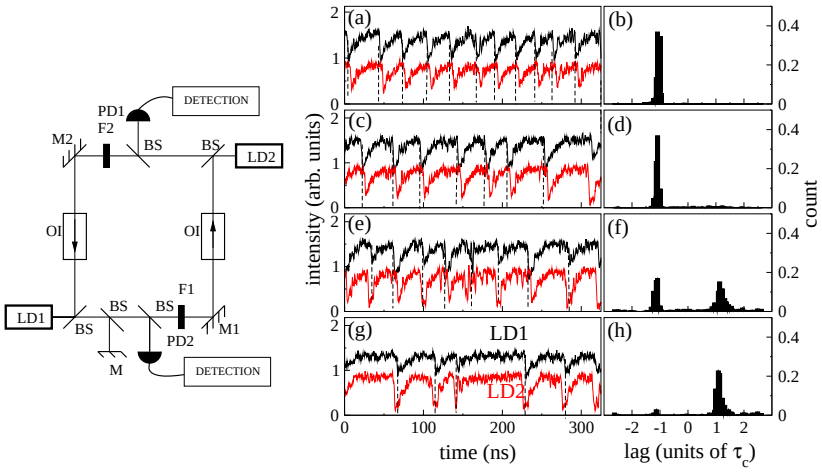

Figure 1.6 Left panel: experimental arrangement of two semiconductor lasers coupled via two independent unidirectional paths. Laser LD1 receives optical feedback from mirror M. Right panel: Experimental output intensities (left column) and the corresponding histogram of time differences between 1000 synchronized dropouts in the two lasers (right column) for increasing transmittance of the filter F2 (from top to bottom). The time traces in the left plots have been shifted vertically for clarity, with LD1 corresponding to the top trace and LD2 to the bottom trace in each plot. Vertical dashed lines in those plots signal the occurrence of a dropout in laser LD1. From Ref. [17].

$\sim \tau_c$), even though a substantial amount of light from LD2 is already entering LD1. For larger back-coupling, however (plot e) laser LD2 begins to have a certain influence and takes over the leader role randomly, leading to a bimodal and symmetric histogram of time differences between dropouts (plot f). The situation resembles that of two mutually coupled lasers without mirrors described above [7], even though that case is perfectly symmetrical and the present one is not, since one of the lasers (LD1) is subject to feedback but not the other. Finally, when the the amount of light being coupled back from LD2 into LD1 is large enough, until the coupling is purely bidirectional (plots g,h), laser LD2 takes over the leader role permanently: its dropouts consistently precede those of LD1, again a time $\sim \tau_c$.

So, naturally, the question arose whether the zero-lag solution always has to be unstable, or whether this can be overcome by modifying the coupling configuration. This question resulted in the extension to a chain of three mutually delay–coupled semiconductor lasers, as discussed in the following section.

1.4 Dynamical relaying as stabilization mechanism for zero-lag synchronization

1.4.1 Laser relay

We have shown in the previous Sections that the natural synchronized state of two delay-coupled lasers is one in which one of the lasers leads the other one a time equal to the flight time between the lasers. However, in many natural situations oscillations between distant dynamical elements can be isochronous even in the presence of non-negligible coupling delays. A specially important example of this phenomenon arises in the nervous system, where zero-lag synchronization has been observed between distant cortical regions [19, 20] and pairwise recordings of neuronal signals [21]. The mechanism of this phenomenon, through which two distant dynamical elements can synchronize at zero lag even in the presence of non-negligible delays in the transfer of information between them, has been debated for many years in the field of neuroscience. Complex mechanisms and neural architectures have been proposed to answer this question [22, 23, 24] that, however, exhibit limitations in the maximum synchronization range (see e.g. [23]), and rely on complex network architectures [24].

Coupling in mutually injected semiconductor lasers is naturally subject to delay. Thus, coupled lasers can be used to explore potential mechanisms for zero-lag synchronization. The left panel of Fig. 1.7 shows a simple mechanism, consisting of three similar dynamical elements coupled bidirectionally in a series, in such a way that the central element acts as a *relay* of the dynamics between the outer elements [25]. The central laser, which does not need to be carefully matched to the other two, mediates their dynamics. Without coupling, the three lasers emit constant power, representing damped relaxation oscillators. In the presence of coupling, the lasers exhibit chaotic outputs that, remarkably, are synchronized with zero lag between the outer lasers, while the central laser either leads or lags the outer lasers. The right panel of Fig. 1.7 shows the time series of the output intensities (left column), in pairs, and the corresponding cross-correlation functions $C_{ij}(\Delta t)$, defined in such a way that a maximal cross-correlation at a positive time difference $\Delta t_{\max}$ indicates that element j is *leading* element i with a time advance $\Delta t_{\max}$, and vice versa. In the situation shown in the figure, the optical frequency of the central laser was slightly decreased with respect to the outer lasers (negatively detuned) by adjusting its temperature, for optimal synchronization quality. Zero-lag synchronization between the intensities of the outer lasers can be clearly seen in Fig. 1.7(a), and also manifests itself in the cross-correlation function shown in Fig. 1.7(d), which presents an absolute maximum at $\Delta t_{\max} = 0$ (i.e. at zero lag). The correlation between the central laser and the outer ones [Fig. 1.7(b,c)] is not as high, and presents a non-zero time lag, as can be seen from the cross-correlation functions shown in Fig. 1.7(e,f). This lag coincides with the coupling time between the lasers. The fact that $\Delta t_{\max}$ is negative means that the central laser dynamically lags the two outer lasers. Therefore, the outer lasers are

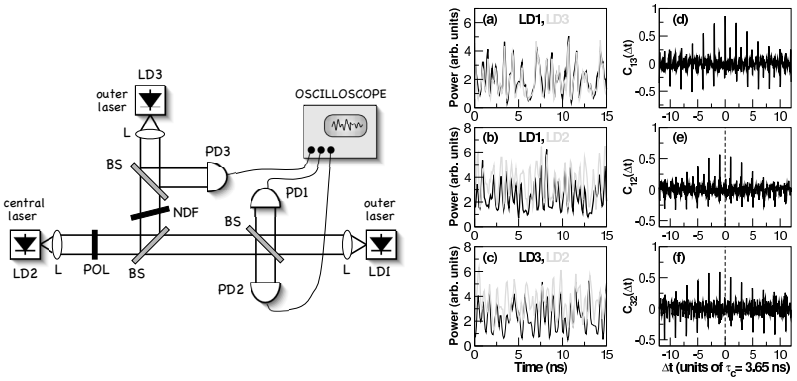

Figure 1.7 Left panel: a central laser (LD2) exchanges information between other two (LD1 and LD3). The coupling time between the central and outer lasers are matched to each other between both branches. Right panel: time series (a-c) and cross-correlation functions (d-f) of the output intensity of the three laser pairs, for a negatively detuned central laser. The time series of the central laser are shifted τ_c for an easier comparison. Adapted from Ref. [25].

not simply driven by the central one. This zero-lag synchronization is quite robust against spectral detuning of the lasers, even for positive detuning (in which case the central laser leads the dynamics).

1.4.2 Mirror relay

A main argument, why zero-lag synchronization could be observed in the laser chain, is that the relay laser in the center is redistributing the signals of the respective outer lasers symmetrically. Consequently, the questions arises whether the central laser could be replaced by a semi- transparent mirror as relay element. The corresponding scheme is depicted in Figure 1.8.

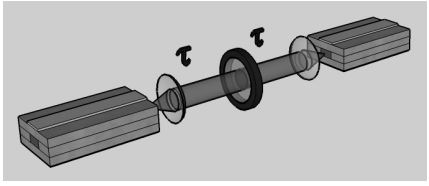

Figure 1.8 Scheme of two mutually delay–coupled lasers with semi-transparent mirror as relay.

The two semiconductor lasers are mutually coupled through a partially transparent mirror placed in the coupling path between both lasers. Therefore, the light injected

into each laser is the sum of its delayed feedback from the mirror and the light coming from the respective other laser. For the numerical studies coupling coefficients and feedback strengths were chosen such that the lasers operate in a chaotic regime. In numerical investigations of this configuration identical synchronization between the dynamics of both lasers was obtained for arbitrary coupling distances between the lasers. For the laser being precisely in the center zero–lag synchronization was found. Changing the position of the mirror turned out not to be relevant for the synchronization quality. Even for strongly asymmetric positioning of the mirror identical synchronization was still observed, then with a temporal offset given by the difference of the corresponding delay times. Thus, identical and even zero–lag synchronization can be achieved with different realizations of the relay element. A parameter which, however, turned out to be critical for the semi- transparent mirror configuration for obtaining good synchronization quality was phase differences between the optical coupling and feedback phases. While the experiments in the all-optical scheme are not easy to sufficiently control REF IDO ET AL. , using electro-optic systems successful identical synchronization could be demonstrated experimentally[**?**].

The results discussed above show that zero-lag synchronization can be achieved in delay-coupled lasers with a relay element in the center. However, it is not clear under which conditions this solution is stable, or whether it is even unconditionally stable due to the common driving of the outer lasers through the relay element. A detailed stability analysis showed the existence of unstable regimes, in particular for not sufficiently strong coupling [**?**]. In addition, it was found that even in large regimes where the synchronization manifold is transversely stable, characterized by negative transverse Lyapunov exponents, still bubbling can occur. Bubbling is the phenomenon of eventual escapes from a synchronization manifold due to an invariant set being transversely unstable. Responsible for the occurrence of bubbling are saddle points, corresponding to destructive interference conditions of the optical field in the outer lasers and the incoupled fields. These saddle points are not only crucial for the onset of the coupling-induced dynamical instabilities, but also for eventual escapes from the synchronization manifold, resulting in bubbling behavior.

1.5
Modulation characteristics of delay-coupled lasers

1.5.1
Periodic modulation

The power dropouts exhibited by a single semiconductor laser with optical feedback, when operating in the regime of low-frequency fluctuations, have been shown to become periodic when an external modulation is applied to the injection current [26, 27] or to the feedback strength [28]. The laser response to an external harmonic modulation, however, is greatly enhanced by coupling [29] (similarly to what is found in general models of nonlinear media [30]). Coupling leads to a very efficient entrainment, which means that less pump current modulation is needed, and thus the modulation

is practically absent in the output of the coupled system (in contrast to what happens in single lasers [26]. Thus in the presence of coupling the low-frequency dropouts are not distorted, but only entrained.

Figure 1.9 shows the response of a system of two optically coupled lasers to a variation of the coupling strength, when one of the lasers is subject to a periodic modulation of its pump current. At the maximum coupling (i.e. when the amount of light that is injected in one laser from the other is maximum given the experimental conditions, top row in the figure), the two lasers are synchronized (only the non-modulated laser output is shown) and perfectly entrained to the periodic signal. For intermediate values of coupling (middle row) the entrainment persists, and only when the coupling strength is reduced more than 50% of its maximum value, the quality of the entrainment is noticeably degraded (bottom row). The results are also given in terms of the probability distribution function of the time intervals between consecutive dropouts. The irregular shape of this function in Fig. 1.9(c) indicates loss of entrainment. Thus, for large enough coupling the response of the two lasers to a pump modulation of one of them is a perfect entrainment, with no direct evidence of the current modulation in the output intensity of either laser, in contrast with the case of a single modulated laser with feedback, in which case the laser is also fully entrained but the current modulation is strongly present in the laser's output [26, 31].

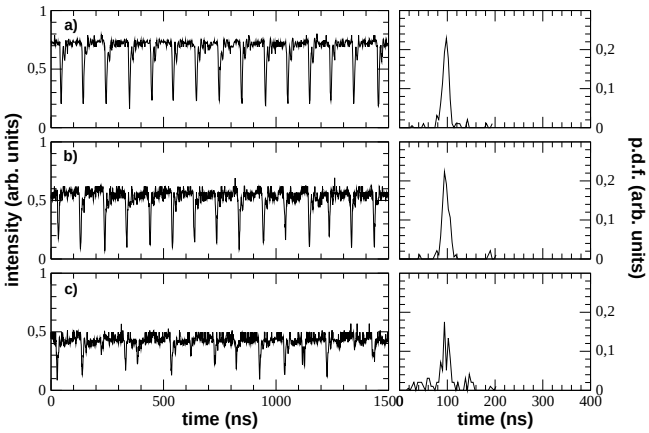

Figure 1.9 Experimental time series of one of two optically coupled lasers, when the coupling between the two lasers is decreased, which is accomplished by placing a neutral density filter between the two lasers. Relative to the maximum coupling: (a) 100%, (b) 83.9% and (c) 45.8%. The right panels show the corresponding probability distribution functions of the intervals between dropouts. From Ref. [31].

It is also interesting to examine the situation in which both lasers are subject to external pump modulation with different frequencies. Let us consider, for instance, the case of two harmonics of a common fundamental f_0, defined by $f_1 = kf_0$ and $f_2 = (k+1)f_0$ with $k > 1$. This is the simplest example of a complex signal, and previous experimental and theoretical studies have shown that certain nonlinear sys-

tems subject to this type of complex signal respond at the fundamental frequency, which is not present in the input. This phenomenon is known as the *missing fundamental illusion*, and has recently been interpreted in terms of an optimal response of excitable systems to a suitable amount of noise, under the name of *ghost stochastic resonance* [32].

Ghost resonant behavior occurring in isolated dynamical elements has been reported experimentally in lasers [33, 34] and electronic circuits [35]. Experiments have shown that the phenomenon also arises in two coupled lasers, both when the lasers are stable in the absence of coupling [36] (so that the power dropouts are induced by coupling), and when the lasers exhibit power dropouts even without coupling [37] (so that the isolated lasers behave as *bona fide* excitable systems [38, 39]). Recent studies in neuronal systems, both theoretical [40, 41] and experimental [42], show that coupling is able to mediate the processing of distributed inputs in networks of neurons (which possess independent dynamics even in the absence of coupling). The experiments that we describe in what follows confirm the existence of this emerging property of excitable networks, using semiconductor lasers with optical feedback as highly controllable excitable systems.

The behavior of a system of two bidirectionally coupled lasers for $k = 2$ and $f_0 = 5$ MHz is shown in Fig. 1.10 for increasing amplitudes of the modulation, assumed equal for both signals. The figure shows the time trace of the intensity of

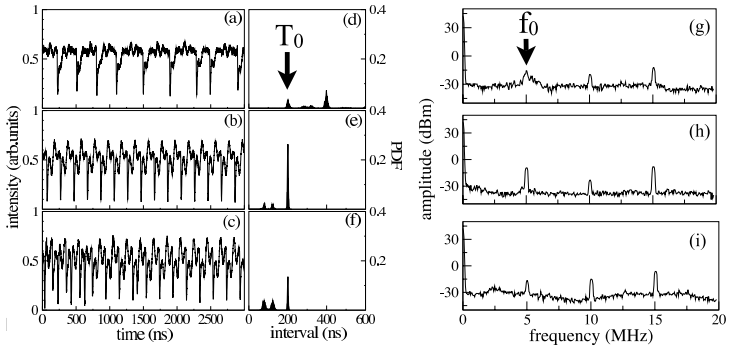

Figure 1.10 Experimental output intensity of one of two coupled lasers (a,b,c), the corresponding probability distribution functions (d,e,f) of the time intervals between consecutive dropouts (right column), and the corresponding RF-spectrum of the output intensity (g,h,i) for increasing values of the modulation amplitude: (a,d,g) $A_1 = A_2 = 0.285$ mA; (b,e,h) $A_1 = A_2 = 0.643$ mA; (c,f,i) $A_1 = A_2 = 0.750$ mA. The input frequencies are $f_1 = 10$ MHz and $f_2 = 15$ MHz, corresponding to inter-pulse periods $T_1 = 100$ ns and $T_2 = 66.7$ ns. The ghost frecuency is $f_0 = 5$ MHz, corresponding to a period $T_0 = 200$ ns. Adapted from Ref. [37].

one of the two lasers on the left, and the probability distribution of the interval between dropouts on the right (the results are basically identical for the other laser, since both lasers are synchronized). The inter-dropout probability distribution is computed from a collection of 1000 dropouts in each case. For a small modulation amplitude (top row in Fig. 1.10) the dropouts occur infrequently at different periods. As the

amplitude grows (middle row), most inter-pulse intervals occur at a definite period T_0 corresponding to the fundamental frequency f_0, which is not present in either of the input signals. For larger amplitudes (bottom row), the input signals take over and dropouts begin to occur at the (larger) input frequencies, reducing the response of the system at the missing fundamental frequency. Therefore, a resonant behavior is observed with respect to the modulation strength: for an intermediate modulation amplitude, the system optimally processes the distributed inputs. We note that this resonance is nontrivially arising from the interplay between the direct electrical modulation of the pump current and the indirect optical driving coming from the other laser.

In the experimental conditions used, the lasers are detuned such that one of them consistently leads the dynamics, with a time lag equal to the coupling time [7]. The behavior of the system does not change if the input modulations are switched between the leader and laggard lasers. It is remarkable that the distributed signals are processed irrespective of this underlying asymmetry in the coupled dynamics.

The subharmonic resonance presented above can also be observed at the level of the RF-spectrum of the lasers' outputs, as shown in the right panels of Fig. 1.10. Peaks of the three frequencies involved, the two (higher) input frequencies $f_1 = 10$ MHz and $f_2 = 15$ MHz and the fundamental frequency $f_0 = 5$ MHz, are clearly observed in the spectrum. The height of the peaks at f_1 and f_2 increases monotonically with the modulation amplitude (from top to bottom), while the peak at f_0 is highest at an intermediate amplitude, which is a clear indicator of a resonance occurring at the missing fundamental frequency [32].

1.5.2 Noise modulation

Over the last decades, much attention in the field of stochastic processes has been paid to the question of how noise can lead to order [43, 44, 45]. In a seminal work, Bryant and Segundo [45] showed that the introduction of white noise in a neuron model produced an invariance in the firing times. In that study, repeating stimulations of the neuron with the same segment of Gaussian-white noise current resulted in a reproducible inter-spike time response. A similar study was made in neocortical neurons of rats by Mainen and Sejnowski [46]. They showed that for constant stimuli the spike trains were imprecise, whereas the introduction of fluctuations in the stimuli, resembling synaptic activity, produced spike trains with reproducible timing. In lasers, a good example of the regularity introduced by noise was given by Uchida et al. [47], who showed the reproducibility of a laser's response to a noisy drive signal. Specifically, a noisy signal was sent repeatedly to a Nd:YAG microchip laser and the system was capable, after a transient, to produce identical response outputs. For small amplitude of the added noise, the outputs are not identical because the relaxation oscillations driven by internal noise dominate the laser output. There is an optimal noise level for which the outputs are identical, because the common-noise-driven signal overcomes the internal noise.

Another constructive effect of noise is inducing the synchronization of coupled

systems. This topic has been studied theoretically in coupled chaotic systems [48, 49, 50], in experimentally in chaotic circuits [51]. The common feature in all these works is that when a certain amount of common noise is introduced, the coupled systems are driven to collapse onto the same trajectory. This property can be used to achieve the isochronal solution in a symmetrical bidirectionally coupled semiconductor laser system, by applying a common source of external noise to the pump current of both lasers (see Fig. 1.11). For large enough noise intensity, the system reaches a common output without lag between them, stabilizing the isochronal solution.

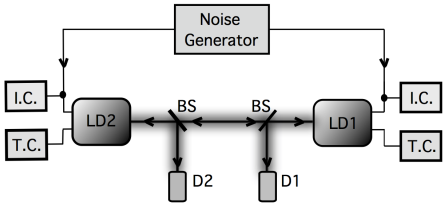

Figure 1.11 Experimental setup leading to noise-induced synchronization. Two semiconductor lasers LD1 and LD2 are coupled by mutual injection, and subject to a common noise source being applied to their pump currents.

The left panel of Fig. 1.12 shows the correlated dynamics of the two lasers when the amount of common noise increases. The temperatures of the lasers are adjusted such that their frequencies are as similar as possible, in order to optimize the mutual injection. The pump currents and the bidirectional alignment are then optimized by looking for the maximum enhancement of the output power due to the mutual injection. The pump currents are fixed slightly above their solitary threshold, for which the lasers operate in the LFF regime. This regime allow for an easy observation and measurement of the isochrony during the experiments.

With the system symmetrically injected, the same noise source is introduced simultaneously into the pump current of the two lasers through an internal bias-T of the laser mounts. In that way, the noise is superimposed to the DC operating level set by the current controller. The left panel of Fig. 1.12 displays the output intensities and the corresponding cross correlation functions for increasing values of the noise level. The output intensities are displaced vertically for clarity, with the top trace representing the output of LD1 and the bottom trace representing LD2. Without noise (plots a and b) LFF dynamics can be observed in the output intensities, and the correspondent cross-correlation function shows a maximum at a lag equal to the flight time τ_c between the lasers. The LFF dynamics starts to disappear as the noise level increases (plot g), even though the cross-correlation still has its maximum at τ_c (plot h). Finally, for a large enough noise level (plot i) a correlation peak arises at zero lag (plot j). These results show that common noise is able to induce zero-lag synchronization in mutually coupled lasers.

The zero-lag synchronized state represented in plots (i,j) of the left panel of Fig. 1.12 are nevertheless markedly different from the intrinsic dynamics of the

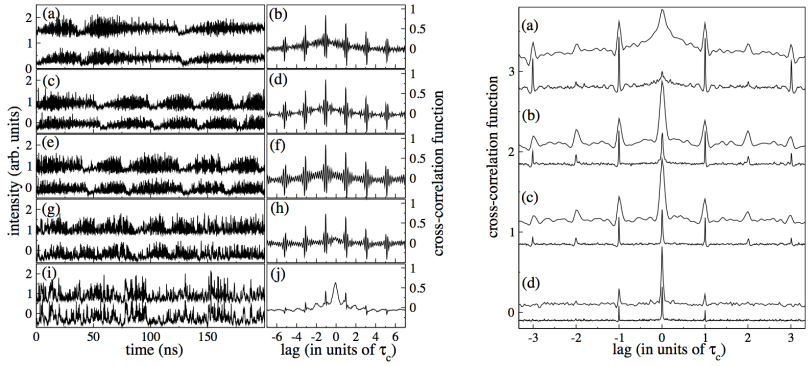

Figure 1.12 Left panel: experimental output intensities (a,c,e,g,i) and corresponding cross correlation functions (b,d,f,h,j) for different values of injected noise level (increasing from top to bottom). Right panel: Numerical cross-correlations functions for filtered (top) and unfiltered (bottom) signals for a fixed noise intensity and varying values of the noise correlation time (decreasing from top to bottom).

lasers. In particular, the cross-correlation of the signals shows a broadening of its maximum peak. In order to determine the origin of this broadening, one can turn to numerical simulations of the system, which allow for an arbitrarily large temporal resolution of the dynamics and an infinite bandwidth of the noise being added to the lasers' pump currents. Indeed, experimental monitoring of the dynamics has a resolution that is strongly limited by the bandwidth of the photodetectors and oscilloscope, and the bandwidth of the common noise is also limited by the frequency filtering characteristics of the bias-T and laser mount. If we ignore bandwidth limitations in our experimental system, we can simulate the output intensities for different noise correlation times and compare the cross-correlation functions for filtered and unfiltered signals, to find a value that shows isochrony for both kinds of signals. The correlation time of the noise is known to play an important role on the dynamics of chaotic lasers [52]. Numerical simulations can be performed on a Lang-Kobayashi-type model of the two mutually coupled lasers [7].

The right panel of Fig. 1.12 shows the cross-correlation functions of the filtered (top traces) and unfiltered (bottom traces) time series of the laser intensities, for decreasing correlation times of the noise. The top trace in (a) corresponds to parameters that approximately match the conditions of the experimental results shown in plots (i,j) of the left panel of Fig. 1.12. The first thing that can be noted is that the zero-lag peak in the cross-correlation is very small in the case of the unfiltered signals (bottom trace in plot a of the right panel of Fig. 1.12). This shows that the noise acts only in the slow dynamics of the system. As the bandwidth of the noise increases (i.e. its correlation time decreases, from top to bottom in the right panel of Fig. 1.12), the zero-lag peak in the cross-correlation of the *unfiltered* time series starts to increase in amplitude with respect to the side peaks, until finally for a small enough time correlation (plot

d) zero-lag synchronization arises not only at slow time scales, but also in the fast dynamics. This confirms that the non-zero correlation time of the noise is the cause of the differences between both types of cross-correlations. For high correlation time of the noise, the system only reacts to the fluctuations in its slow dynamics, whereas in the limit of very low noise correlation time both dynamics can respond, for the same noise strength.

1.5.3
Application: key exchange protocol

Coupled semiconductor lasers play an important role in many applications. Among them longitudinal coupled-cavities lasers (e.g., C^3 lasers) have been used for spectral selection; coherent coupling allows for high output power with good spectral and beam properties; laterally-coupled laser arrays have been realized to also achieve coherent coupling. As presented in the previous sections, a delay in the coupling path introduces dynamical instabilities and particular synchronization properties which can be harnessed for applications. Here, we would like to give a brief perspective of suggested or foreseen applications. Delayed–coupling configurations are being considered for applications in encrypted communication. In [**?**] a novel key exchange protocol has been suggested, utilizing the synchronization properties of two mutually delay–coupled semiconductor lasers with the semi-transparent mirror as relay element.

MIGUEL, CAN YOU ELABORATE ON THIS?

Finally, networks of delay-coupled lasers are currently being studied for the realization of novel information processing concepts, being inspired by neuronal systems. They are expected to represent a suitable reservoir for the realization of a Liquid State Machine. This illustrates that delay effects might become very useful, improving existing applications or allowing for novel applications.

1.6
Conclusion

Delay-coupled semiconductor lasers show a rich phenomenology of dynamical properties and synchronization scenarios. They represent well-controllable test-beds to study these systems which are being recognized to be of interest in more and more areas of science.

PLEASE MORE

In addition, we illustrated the application potential of the reported configurations.

PLEASE MORE

The configurations discussed in this chapter represent only a few possibilities among many more. Motivated by the described coupling configurations, more complicated network arrangement of many delay–coupled lasers or other delay-coupled oscillators could be relaized. They represent a very promising and challenging field of study. These approaches might help us to understand certian aspects of brain

dynamics, and even more to explore and realize bio-inspired concepts of information processing like Reservoir Computing.

Acknowledgements The authors would like to thank many collaborators and institutions, who contributed to the reported work, through their intellectual and financial help. They would like to express many thanks to Claudio Mirasso, Michael Peil, Tilmann Heil, Wolfgang Elsäßer, Jan Danckaert, Raul Vicente, Guy Van der Sande, Thomas Erneux, Javier Martin-Buldu, Rajarshi Roy, Atsushi Uchida. Part of the work was funded via the different research programs from the European Community in FP5, FP6, and FP7 (Projects OCCULT, GABA, PHOCUS), the Spanish MICINN under Project No. TEC2009-14101 DeCoDicA, the German Research Foundation, the Volkswagen Foundation, and the German BMBF.

Bibliography

1 Botez, D. and Scifres, D. (eds) (1994) *Laser Diode Arrays*, Cambridge Studies in Modern Optics, Cambridge University Press.

2 Wieczorek, S., Krauskopf, B., Simpson, T., and Lenstra, D. (2005) The dynamical complexity of optically injected semiconductor lasers. *Phys. Rep.*, **416**, 1–128.

3 DeFreez, R., Bossert, D., YU, N., K., H., R.A., E., and Winful, H. (1988) Spectral and picosecond temporal properties of flared guide y-coupled phase-locked laser arrays. *Applied Physics Letters*, **53**, 2380–2382.

4 Merbach, D., Hess, O., Herzel, H., and Schll, E. (1995) Injection-induced bifurcations of transverse spatiotemporal patterns in semiconductor laser arrays. *Physical Review E*, **52**, 15711578.

5 Winful, H.G. and Rahman, L. (1990) Synchronized chaos and spatiotemporal chaos in arrays of coupled lasers. *Phys. Rev. Lett.*, **65**, 1575–1578.

6 Hohl, A., Gavrielides, A., Erneux, T., and Kovanis, V. (1997) Localized synchronization in two coupled nonidentical semiconductor lasers. *Physical Review Letters*, **78** (25), 4745–4748. URL http://link.aps.org/doi/10.1103/PhysRevLett.78.4745.

7 Heil, T., Fischer, I., Elsässer, W., Mulet, J., and Mirasso, C.R. (2001) Chaos synchronization and spontaneous symmetry-breaking in symmetrically delay-coupled semiconductor lasers. *Physical Review Letters*, **86** (5), 795–798.

8 Fujino, H. and Ohtsubo, J. (2001) Synchronization of chaotic oscillations in mutually coupled semiconductor lasers. *Opt. Rev.*, **8**, 351–357.

9 Wünsche, H.J., Bauer, S., Kreissl, J., Ushakov, O., Korneyev, N., Henneberger, F., Wille, E., Erzgräber, H., Peil, M., Elsäß er, W., and Fischer, I. (2005) Synchronization of delay-coupled oscillators: A study of semiconductor lasers. *Physical Review Letters*, **94** (16), 163 901 1–4, doi:10.1103/PhysRevLett.94.163901. URL http://link.aps.org/doi/10.1103/PhysRevLett.94.163

10 Mulet, J., Mirasso, C., Heil, T., and Fischer, I. (2004) Synchronization scenario of two distant mutually coupled semiconductor lasers. *Journal of Optics B: Quantum and Semiclassical Optics*, **6** (1), 97–105, doi:10.1088/1464-4266/6/1/016. URL http://stacks.iop.org/1464-4266/6/i=1/a=016?key=c

11 Lang, R. and Kobayashi, K. (1980) External optical feedback effects on semiconductor laser properties. *IEEE Journal of Quantum Electronics*, **QE-16**, 347–355.

12 Locquet, A., Masoller, C., and Mirasso, C.R. (2002) Synchronization regimes of optical-feedback-induced chaos in unidirectionally coupled semiconductor lasers. *Phys. Rev. E*, **65**, 056 205.

13 Locquet, A., Masoller, C., MÈgret, P., and Blondel, M. (2002) Comparison of two types of synchronization of external-cavity semiconductor lasers. *Opt. Lett.*, **27**, 31–33.

14 Masoller, C. (2001) Anticipation in the synchronization of chaotic semiconductor lasers with optical feedback. *Phys. Rev. Lett.*, **86**, 2782–2785.

15 Sivaprakasam, S., Shahverdiev, E.M., Spencer, P.S., and Shore, K.A. (2001) Experimental demonstration of anticipating synchronization in chaotic semiconductor

lasers with optical feedback. *Phys. Rev. Lett.*, **87**, 154 101.

16 Ávila, J.F.M., Vicente, R., Rios Leite, J.R., and Mirasso, C.R. (2007) Synchronization properties of bidirectionally coupled semiconductor lasers under asymmetric operating conditions. *Phys. Rev. E*, **75**, 066 202.

17 Gonzalez, C.M., Torrent, M.C., and Garcia-Ojalvo, J. (2007) Controlling the leader-laggard dynamics in delay-synchronized lasers. *Chaos*, **17** (3), 033 122, doi:10.1063/1.2780131. URL http://link.aip.org/link/?CHA/17/033122/1.

18 Uchida, A., Rogister, F., Garcìa-Ojalvo, J., Roy, R., and Wolf, E. (2005) *Synchronization and communication with chaotic laser systems*, Elsevier, vol. Volume 48, pp. 203–341.

19 Engel, A., Konig, P., Kreiter, A., and Singer, W. (1991) Interhemispheric synchronization of oscillatory neuronal responses in cat visual cortex. *Science*, **252** (5009), 1177–1179.

20 Roelfsema, P.R., Engel, A.K., Konig, P., and Singer, W. (1997) Visuomotor integration is associated with zero time-lag synchronization among cortical areas. *Nature*, **385** (6612), 157–161.

21 Schneider, G. and Nikolic, D. (2006) Detection and assessment of near-zero delays in neuronal spiking activity. *Journal of Neuroscience Methods*, **152** (1-2), 97–106.

22 Traub, R.D., Whittington, M.A., Stanford, I.M., and Jefferys, J.G.R. (1996) A mechanism for generation of long-range synchronous fast oscillations in the cortex. *Nature*, **383** (6601), 621–624.

23 König, P., Engel, A.K., and Singer, W. (1995) Relation between oscillatory activity and long-range synchronization in cat visual cortex. *Proceedings of the National Academy of Sciences of the USA*, **92** (1), 290–294.

24 Bibbig, A., Traub, R.D., and Whittington, M.A. (2002) Long-range synchronization of γ and β oscillations and the plasticity of excitatory and inhibitory synapses: a network model. *Journal of Neurophysiology*, **88** (4), 1634–1654.

25 Fischer, I., Vicente, R., Buldú, J.M., Peil, M., Mirasso, C.R., Torrent, M.C., and García-Ojalvo, J. (2006) Zero-lag long-range synchronization via dynamical relaying. *Physical Review Letters*, **97** (12), 123 902.

26 Sukow, D.W. and Gauthier, D.J. (2000) Entraining power-dropout events in an external-cavity semiconductor laser using weak modulation of the injection current. *IEEE Journal of Quantum Electronics*, **36** (2), 175–183.

27 Buldú, J.M., García-Ojalvo, J., Mirasso, C.R., and Torrent, M.C. (2002) Stochastic entrainment of optical power dropouts. *Physical Review E*, **66** (2), 021 106.

28 Lam, W., Guzdar, P.N., and Roy, R. (2003) Effect of Spontaneous Emission Noise and Modulation on Semiconductor Lasers Near Threshold with Optical Feedback. *International Journal of Modern Physics B*, **17**, 4123–4138.

29 Buldu, J.M., Vicente, R., Perez, T., Mirasso, C.R., Torrent, M.C., and Garcia-Ojalvo, J. (2002) Periodic entrainment of power dropouts in mutually coupled semiconductor lasers. *Applied Physics Letters*, **81** (27), 5105–5107.

30 Lindner, J.F., Meadows, B.K., Ditto, W.L., Inchiosa, M.E., and Bulsara, A.R. (1995) Array enhanced stochastic resonance and spatiotemporal synchronization. *Physical Review Letters*, **75** (1), 3–6.

31 Buldú, J.M., García-Ojalvo, J., Torrent, M.C., Vicente, R., Pérez, T., and Mirasso, C.R. (2003) Entrainment of optical low-frequency fluctuations is enhanced by coupling. *Fluctuations and Noise Letters*, **3** (2), L127–L136.

32 Chialvo, D.R. (2003) How we hear what is not there: A neural mechanism for the missing fundamental illusion. *Chaos*, **13** (4), 1226–1230.

33 Buldú, J.M., Chialvo, D.R., Mirasso, C.R., Torrent, M.C., and García-Ojalvo, J. (2003) Ghost resonance in a semiconductor laser with optical feedback. *Europhysics Letters*, **64** (2), 178.

34 Van der Sande, G., Verschaffelt, G., Danckaert, J., and Mirasso, C.R. (2005) Ghost stochastic resonance in vertical-cavity surface-emitting lasers: Experiment and theory. *Physical Review E*, **72** (1), 016 113.

35 Calvo, O. and Chialvo, D.R. (2006) Ghost

stochastic resonance in an electronic circuit. *International Journal of Bifurcation and Chaos*, **16** (3), 731–735.

36 Buldu, J.M., Gonzalez, C.M., Trull, J., Torrent, M.C., and Garcia-Ojalvo, J. (2005) Coupling-mediated ghost resonance in mutually injected lasers. *Chaos*, **15** (1), 013 103, doi:10.1063/1.1827412.

37 González, C.M., Buldú, J.M., Torrent, M.C., and García-Ojalvo, J. (2007) Processing distributed inputs in coupled excitable lasers. *Physical Review A*, **76** (5), 053 824.

38 Giudici, M., Green, C., Giacomelli, G., Nespolo, U., and Tredicce, J.R. (1997) Andronov bifurcation and excitability in semiconductor lasers with optical feedback. *Physical Review E*, **55** (6), 6414–6418.

39 Mulet, J. and Mirasso, C.R. (1999) Numerical statistics of power dropouts based on the lang-kobayashi model. *Physical Review E*, **59** (5), 5400–5405.

40 Balenzuela, P. and Garcia-Ojalvo, J. (2005) Neural mechanism for binaural pitch perception via ghost stochastic resonance. *Chaos*, **15** (2), 023 903.

41 Balenzuela, P., Garcia-Ojalvo, J., Manjarrez, E., Martínez, L., and Mirasso, C.R. (2007) Ghost resonance in a pool of heterogeneous neurons. *Biosystems*, **89** (1-3), 166–172.

42 Manjarrez, E., Balenzuela, P., García-Ojalvo, J., Vásquez, E.E., Martínez, L., Flores, A., and Mirasso, C.R. (2007) Phantom reflexes: Muscle contractions at a frequency not physically present in the input stimuli. *Biosystems*, **90** (2), 379–388.

43 Horsthemke, W. and Lefever, R. (1984) *Noise Induced Transitions*, Springer.

44 Garcia-Ojalvo, J. and Sancho, J. (1999) *Noise in Spatially Extended Systems*, Springer.

45 Lindner, B., GarcÌa-Ojalvo, J., Neiman, A., and Schimansky-Geier, L. (2004) Effects of noise in excitable systems. *Physics Reports*, **392** (6), 321–424.

46 Mainen, Z.F. and Sejnowski, T.J. (1995) Reliability of spike timing in neocortical neurons. *Science*, **268** (5216), 1503–1506.

47 Uchida, A., McAllister, R., and Roy, R. (2004) Consistency of nonlinear system response to complex drive signals. *Phys. Rev. Lett.*, **93** (24), 244 102.

48 Maritan, A. and Banavar, J.R. (1994) Chaos, noise, and synchronization. *Phys. Rev. Lett.*, **72** (10), 1451–1454.

49 Toral, R., Mirasso, C.R., Hernández-García, E., and Piro, O. (2001) Analytical and numerical studies of noise-induced synchronization of chaotic systems. *Chaos*, **11**, 665–673.

50 Zhou, C. and Kurths, J. (2002) Noise-induced phase synchronization and synchronization transitions in chaotic oscillators. *Phys. Rev. Lett.*, **88**, 230 602.

51 Sánchez, E., Matías, M.A., and Pérez-Muñuzuri, V. (1997) Analysis of synchronization of chaotic systems by noise: An experimental study. *Phys. Rev. E*, **56**, 4068–4071.

52 Buldú, J.M., García-Ojalvo, J., Mirasso, C.R., Torrent, M.C., and Sancho, J.M. (2001) Effect of external noise correlation in optical coherence resonance. *Phys. Rev. E*, **64** (5), 051 109.